Available online at www.sciencedirect.com
SCIENCE DIRECT
Catalysis Today 105 (2005) 680–688
CATALYSIS TODAY
www.elsevier.com/locate/cattod

Research of mass-transfer in fibrous sorption-active materials

O.V. Chub [a,*], E.S. Borisova [a], O.P. Klenov [a], A.S. Noskov [a], A.V. Matveev [b], I.V. Koptyug [b]

[a] *Boreskov Institute of Catalysis, Novosibirsk, Russia*
[b] *International Tomography Center, Novosibirsk, Russia*

Abstract

The mass-transfer processes in fiberglass were studied in the course of drying the saturated glass fabric sample. Experiments were carried out using an Avance DRX Bruker spectrometer equipped with a micro tomography device. Experimental signal intensities of fluids flowing at different velocities were obtained. A one-dimensional mathematical model was applied to calculate mass-transfer coefficients from experimental data. Dependencies Nu(*Re*) at the Reynolds number varied between 0 and 400 were obtained at different fluid velocities. The data obtained were compared to correlation dependencies for woven Pt/Pd gauzes and for rows of parallel cylinders. Numeric experiments of gas flow filtration at low Reynolds numbers ($Re < 1$) were carried out using the CFD FLUENT software package. Fibrous material was represented as porous system consisting of bunches of parallel cylinders with varied distances between the cylinders. Dependence Nu(*Re*) was calculated at various parameters of system.

Keywords: Mass-transfer; Sorption-active materials; Reynolds number

1. Introduction

Since the early 20th century, porous materials have been applied for numerous chemical processes and, for this reason, the fluid and gas flowing through the systems has been the subject of long-term investigations. Since early 1940's, a number of works have been devoted to the flows through grain layers. Even though fibrous materials, in particular woven fabrics, have been of considerable interest that time, the studies in the field has been far less in number. These studies have mainly dealt with hydrodynamic problems but not with heat and mass transfer [1], while the application of metal gauzes for industrial processes of ammonia oxidation has made it necessary to develop methods for calculation of heat exchange parameters in the systems [2]. At present, woven materials, such as fiberglasses are used as catalyst supports in sorption [1] and catalytic processes [3]. Therefore, the problem of quantifying mass transfer coefficients in the reaction systems is of vital importance.

The present work is devoted to studying mass transfer in a microporous fibrous structure with a glass fiber as an example and to establishing the criterial dependencies Nu(*Re*) in the Reynolds number range between 0 and 400. NMR tomography was used for the experimental studies. The CFD FLUENT6.1.12 software package and a specially developed mathematical model were used for the calculations.

2. Description of glass fiber geometry

An optical electron microscope REM-100U was used to characterize the glass fiber structure (the weave pattern, arrangement and geometrical size of yarns). Fig. 1 shows fabric micrographs acquired at different resolutions: the mode of yarn interlacing (Fig. 1a) and the fiber geometry (Fig. 1b). The microscopic data are used to determine the mean fiber diameter in the yarn and the mean distance

* Corresponding author.
E-mail address: sumenk@catalysis.nsk.su (O.V. Chub).

0920-5861/$ – see front matter © 2005 Elsevier B.V. All rights reserved.
doi:10.1016/j.cattod.2005.06.049

Nomenclature and abbreviations

C	concentration of fluid vapor in gas phase (g/m^3)
$\bar{C}$	mean integral gas-phase concentration of fluid vapor in the sample (g/m^3)
C_p	specific heat capacity of gas mixture (J/(g K))
C_S	saturated concentration of fluid (water) vapor on the fabric surface, g/m^3
d	yarn diameter (m)
d_0	fiber diameter (m)
$D(\hat{T})$	coefficient of water vapor diffusion in air (m^2/s)
ΔH	specific heat of evaporation (J/g)
$L = 2d$	glass fabric thickness (m)
R_0	average rate of fluid evaporation from the sample corresponding to linear section of curve obtained experimentally (g/(m^3 s))
$R(z)$	rate of fluid evaporation from the sample variable to the sample thickness (g/(m^3 s))
S_{ud}	specific surface area (m^2/m^3)
$\bar{T}$	mean integral gas temperature in the sample (K)
T	gas temperature (K)
T_0	inlet gas temperature (K)
u	linear velocity of gas flow (m/s)
z	coordinate along the sample length (m)

Greek letters

α	heat transfer coefficient (J/(m^2 s K))
β	mass transfer coefficient (m/s)
ε	fabric porosity
θ	solid phase (sample) temperature (K)
$\lambda(T)$	coefficient of heat conductivity of gas mixture (W/m K)
$\nu(T)$	viscosity of gas mixture (air) (m^2/s)
ρ	gas density (mol/m^3)

between fibers. Fig. 1a demonstrates some ordered and comparatively uniform arrangement of the fibers. Basic characteristics of the fabric are given in Table 1.

The surface area of the sample was calculated from the isotherm of nitrogen adsorption at 77 K; the data were obtained using an ASAP 2400 Micromeritics instrument. The sample was established to have a comparatively small external surface area (Table 1).

3. Methods for studying mass-transfer processes in a glass fabric

3.1. Experimental studies of the mass transfer processes

The mass transfer process was studied in the course of drying of a fabric sample. Before being used, the sample was uniformly impregnated with a fluid. The parameter to be determined was the rate of evaporation of a model fluid (R_0) from the external yarn surface. The determined evaporation rate allowed the intensity of processes to be identified in the sample under study.

Substances with various physicochemical properties were chosen as model fluids; these were water, dioxane and benzyl alcohol. The fluid amount at every instant was measured in situ using an Avance DRX Bruker spectrometer equipped with a micro tomography device. A schematic of the experimental setup is shown in Fig. 2.

The fabric sample was pre-calcined at $T = 900$ °C before experiments in order to clean the surface from virtual organic impurities. In each run, a model fluid (100 μl) was added from a pipette to the calcined sample. The impregnated sample was mounted on a supporting capron gauze in a cylindrical flow reactor (the reactor internal diameter and the sample diameter equal 2×10^{-2} m) and blown by dry air (relative humidity 0.1%) at some given constant consumption. During drying, the NMR signal was recorded from protons of the fluid saturating the sample. In each run, time dependence of the signal intensities was obtained; the dependences were normalized with respect to the maximal (100% fluid content in the sample) and minimal (the dry sample) values. The obtained experimental results allowed us to turn from formal parameters (NMR signal intensity) to the physical interpretation of the data (evaporation rates, Fig. 3a–c). A series of experiments were carried out with each of the model fluids at the air consumption varied from 8.53×10^{-5} to 4.24×10^{-4} m^3/s.

The experiments illustrated in Fig. 3a–c are evidences of comparatively slow fluid evaporation from the fabric surface, when the air blows at low linear velocities, and of an increase in the evaporation rate with an increase in the inlet air consumption. The rate of sample drying (R_0) is determined from the tangent to the rectilinear fragment in each of the drying rate curve. The stationary mode (u = const) is assumed for the drying process, which is limited by the external mass exchange (the rate of a substance feeding to the external evaporation surface equals the evaporation rate).

Two-dimensional patterns of water and benzyl alcohol distribution through the fabric surface (Fig. 4a and b) allow the system 'fibrous support-fluid' to be visualized before the drying, and provide additional information on the fluid distribution in the system. The initial fluid distribution through the sample is illustrated in Fig. 4a and b, where the thickness integrated fluid quantity is indicated by a specific color. The cellular-like distribution is visual, which replicates the yarn structure in the fabric. Evidently, all the yarns are rather uniformly saturated with the liquid due to capillary effects.

The experimental evaporation rates (R_0) obtained by the said method were used as an input parameter in the mathematical model to calculate the mass exchange coefficient $\beta(u)$.

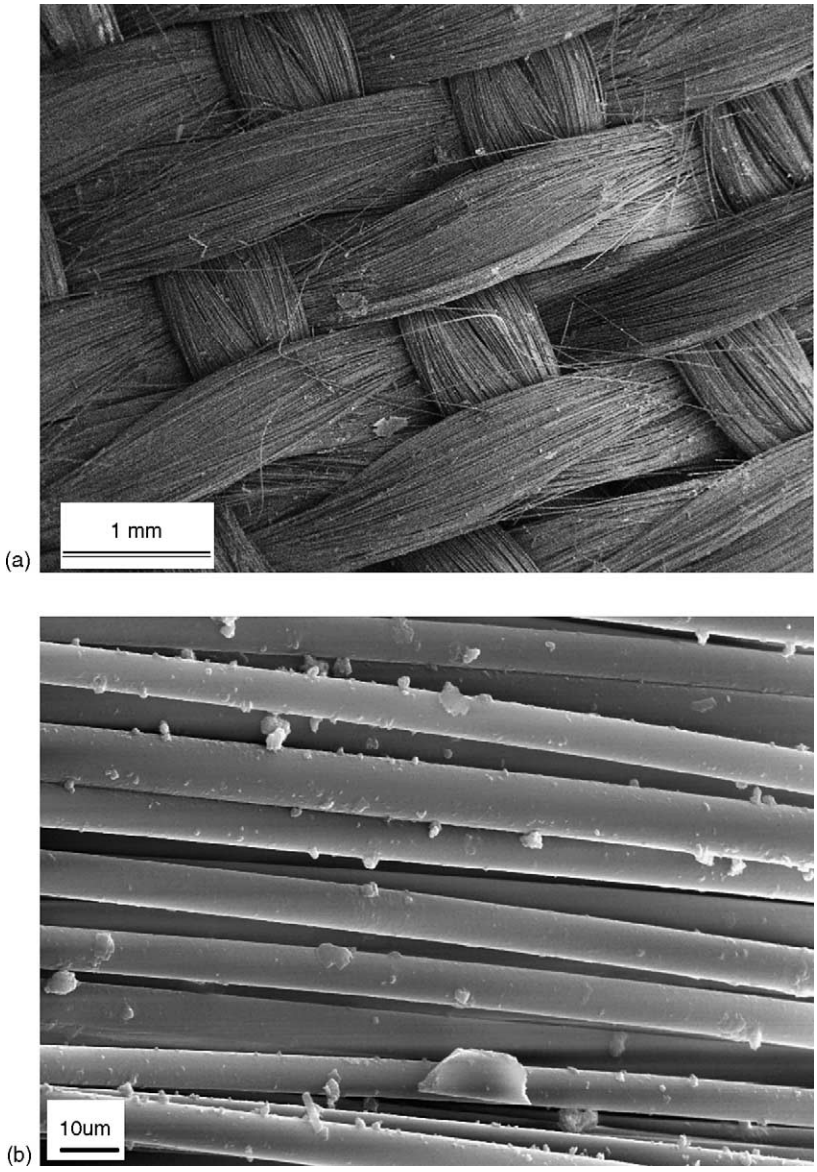

Fig. 1. The photos of fiberglass sample. (a) The mode of yarns interlacing; (b) fiber geometry.

3.2. Mathematical model

A one-dimensional mathematical model is formulated (Appendix A) for description of the stationary process of fluid evaporation from a fiberglass fabric.

Variations in the fabric and air temperatures during drying are taken into account in the model. While identifying starting conditions, the concentration of the fluid vapor is assumed equal to zero in the gas phase, and the initial process temperature equal to the inlet gas flow temperature as it is measured in each run.

The results obtained by processing experimental data in terms of the proposed mathematical model are illustrated in Fig. 5a–c. These are external mass transfer coefficients (Sherwood criterion, Sh) depend upon airflow rate (expressed in terms of the Reynolds criterion, *Re*) assuming that the yarns are impermeable. Mass transfer coefficients calculated for one and two rows of cylinders by the formulae known from literature [4], as well as the ones calculated by the experimental formula $Sh = 0.45+0.55Re^{1/2}Sc^{1/3}$ [5] for platinum gauzes are shown for comparison.

Emphasize that the Reynolds number, *Re*, is calculated here using the yarn diameter as characteristic size; it is approximately 0.75 mm for the fiberglass, and the calculated specific surface of evaporation equals 4275 m^2/m^3.

In the case under consideration, the mass transfer is only taken into account for gas flowing around yarns. It is assumed that each yarn of the fabric is impermeable, and the evaporation occurs at the surface of external yarns. Therefore, the contribution of local mass transfer to the flowing around yarns is not taken into account. At the gas flow rate varied in a certain range in the experiments, *Re* varies from 0 to 400. When gas flows at the rate more than 1 m/s, the local mass transfer inside the yarns may contribute more considerably to

Table 1
Fiberglass characteristics

Parameters	
Distance between fibers in the yarn (μm)	3–4
Fiber diameter (μm)	6.5
Yarn diameter (μm)	750
Number of warp yarns (1/cm)	13
Number of weft yarns (1/cm)	14
BET surface area (m^2/g)	0.1802

the total mass transfer, which is determined as a sum of the external (flowing around a conditionally impermeable yarn) and internal (flowing around fibers inside the yarn) mass transfer. We have assessed the total mass transfer based on numerical modeling with the CFD Fluent software to take into account the local hydrodynamics of a flow around fibers in the yarns of the fabric.

3.3. Calculation of heat transfer coefficients for the fabric model based on the direct solution of the hydrodynamic equation

A simplified model of the glass fabric was used for the calculation. The sample under study was considered as two rows of parallel cylinder bundles in a certain mutual special arrangement (Fig. 6). The distance between cylinders in the bundles was assumed constant and equal to 4 μm at the fiber diameter of 6.5 μm, the number of elements being 67 in each bundle at their five-row order. Geometrically, the neighboring cells formed equilateral triangles. Variable parameters in the model were interbundle distance (A is the size of transport channels, see Fig. 6) and flow rate. The calculations were done for the laminar flow mode. The filtered flow was air at the temperature taken equal to T_a = 300 K. The yarn temperature was constant, T_y = 320 K. For each fiber, a surface averaged heat transfer coefficient was determined in terms of the Nusselt criterion, Nu(u), then averaged Nu(u) values were determined for the external surface of the whole yarn.

The velocity and temperature distribution, according to the model of the glass fabric (Fig. 6) for the inter-yarn distance 10 μm, is showed on Figs. 7 and 8. The calculated data on Nu for separate fibers, limited to the dotted line rectangle on the temperature map (Fig. 8), are shown as histograms Fig. 9. The value of superficial velocity was 2.5 m/s.

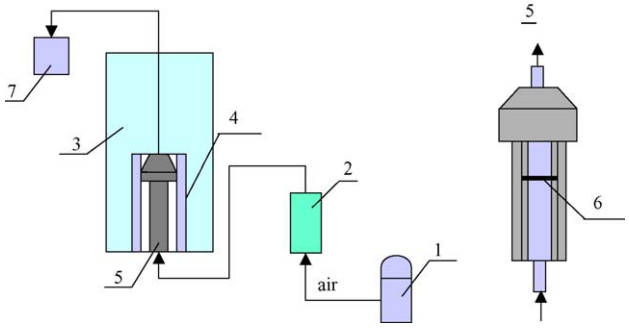

Fig. 2. Scheme of NMR setup. 1, compressor; 2, rotameter; 3, magnet; 4, radiofrequency coil; 5, cell; 6, sample; 7, hygrometer.

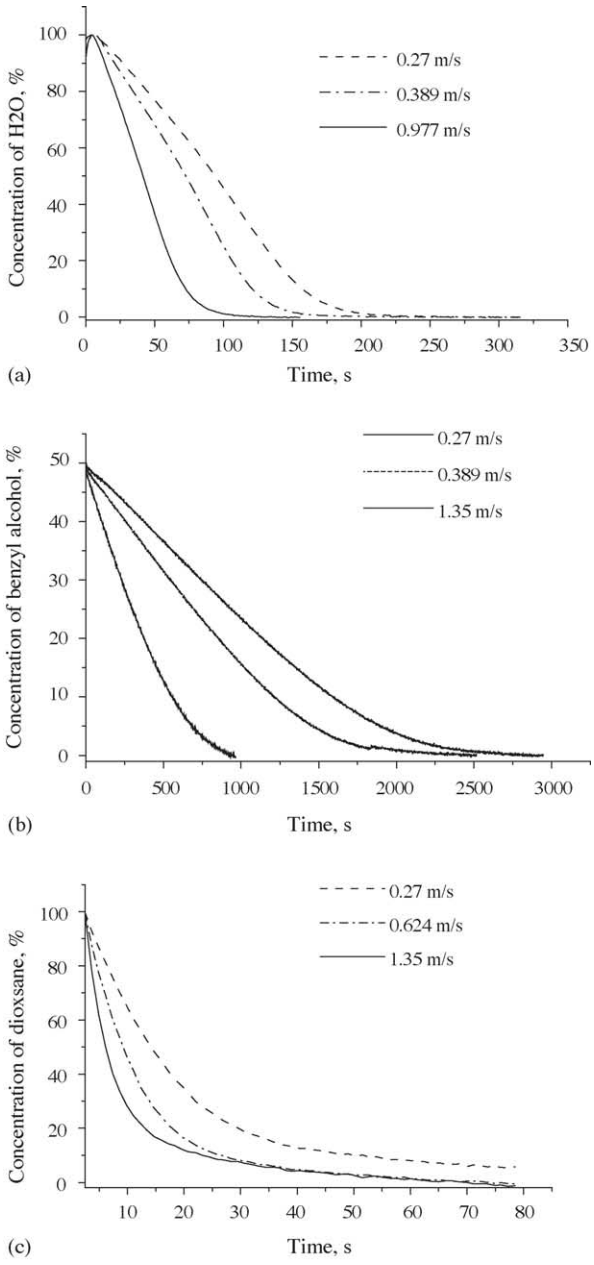

Fig. 3. Fiberglass sample drying curves: (a) impregnated with water; (b) impregnated with benzyl alcohol; (c) impregnated with dioxane.

The results illustrated in Figs. 7–9 indicate the predominant contribution of the fibers located at the fabric surface to heat transfer in the flow. The Nusselt numbers differ by 7–9 orders of magnitude for the fibers inside and outside the yarns but the difference reduces as the filtration rate increases. In addition, the contribution of the fibers, which are on the fiber surface along intra-fabric transport channels, augments as a result of increasing the flow rate. These facts argue that an increase in the inlet rate leads to the flow redistribution between transport channels between the yarns and filtration through the yarns.

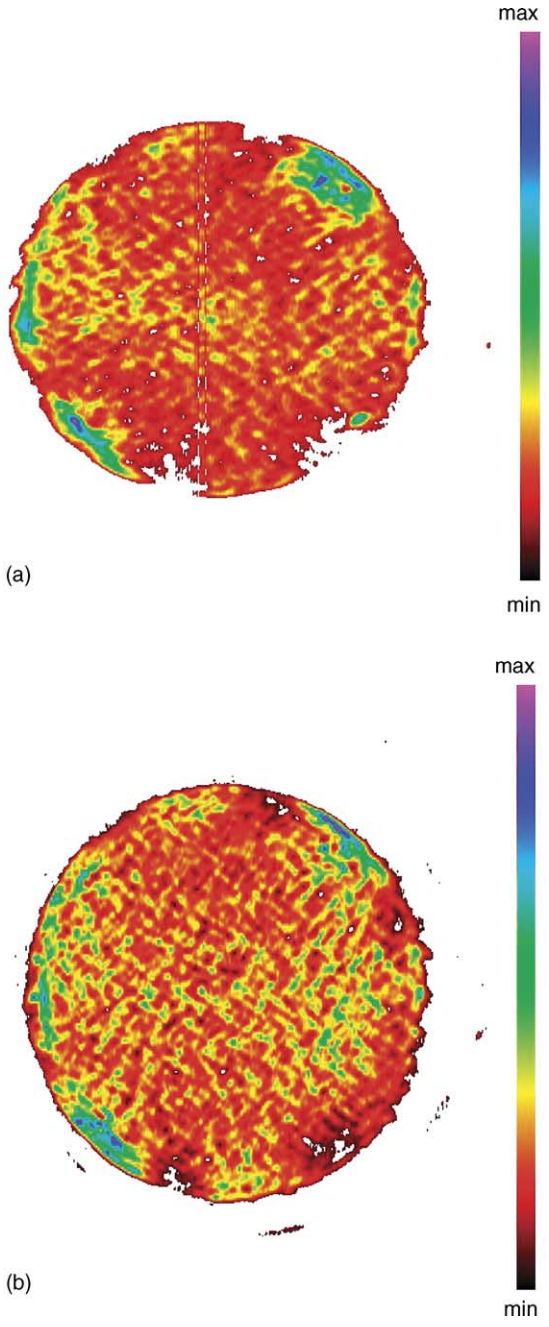

Fig. 4. Distribution of liquids through the sample surface.

The data on local Nusselt numbers of individual fibers were used to determine the sample averaged values for Nu(Re_0). The calculations were based on two models of fabric with transport channels of 5 and 10 μm in size (parameter A in Fig. 6). The fiber diameter $d_0 = 6.5$ μm was used as the characteristic size to determine Re_0. Fig. 10 illustrates the calculation results, as well as the experimental dependencies Nu(Re_0) that are obtained by conversion (based on the similarity of heat and mass transfer processes) of the Sherwood numbers Sh(Re) determined experimentally from fluid evaporation.

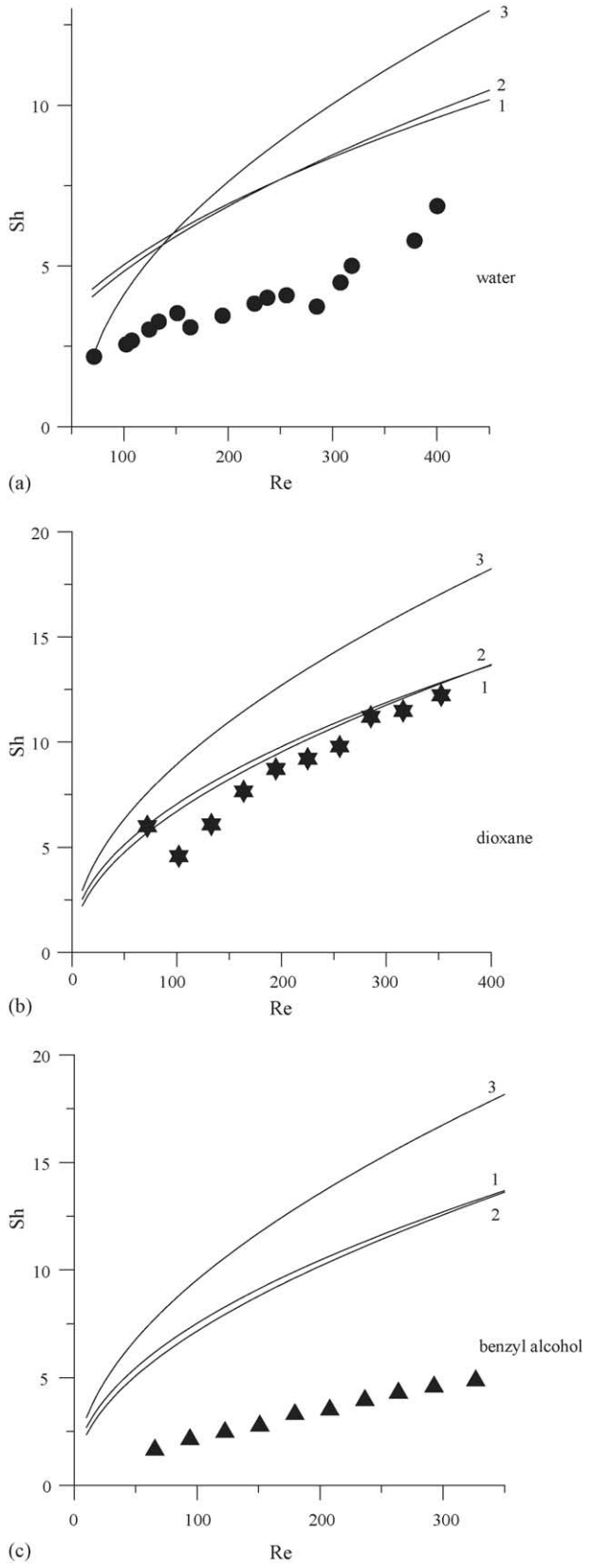

Fig. 5. Dependence of Sh on Re as compared to the known formulae for metal gauzes (1) [5], for one row of cylinders (2) for two rows of staggered cylinders (3).

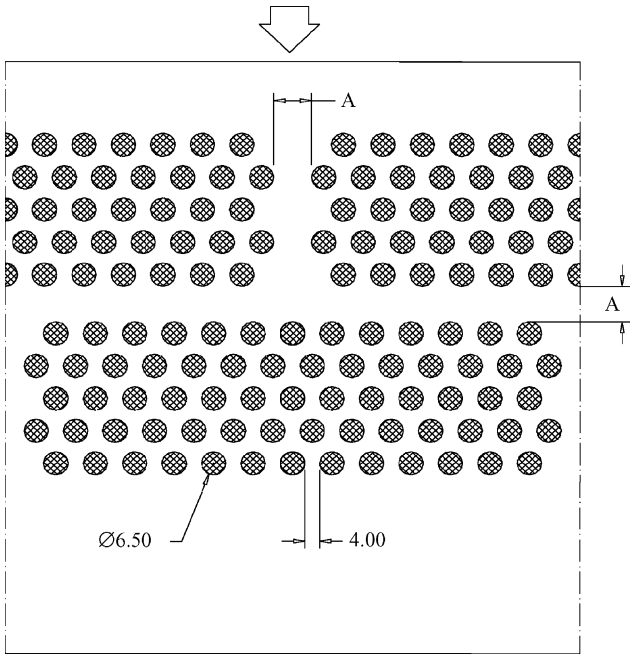

Fig. 6. Geometry of a simplified model of glass fabric.

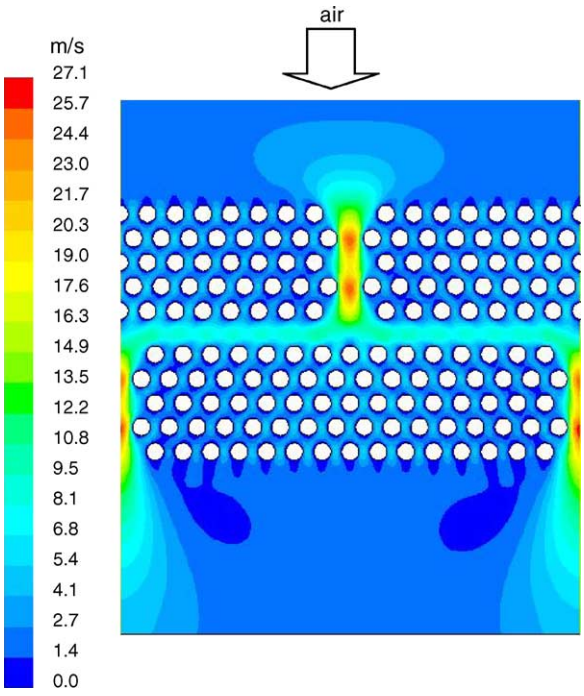

Fig. 7. The velocity distribution on the model of the glass fabric.

4. Discussion

The inspection of Fig. 10 shows that the results on calculation of heat transfer parameters for the woven fabric in terms of the comparatively simple 2D model coincide satisfactorily with the main array of experimental data on water evaporation. The top boundary for the experimental points is formed by the data calculated in terms of the model with 10 μm transport channels, while the data for the model with 5 μm channels fit the bottom boundary. This may be indirect evidence that, irrespective of the complex 3D weave geometry (see Fig. 1a), the transport channels between the yarns in the fabric are 5 and 10 μm in characteristic size.

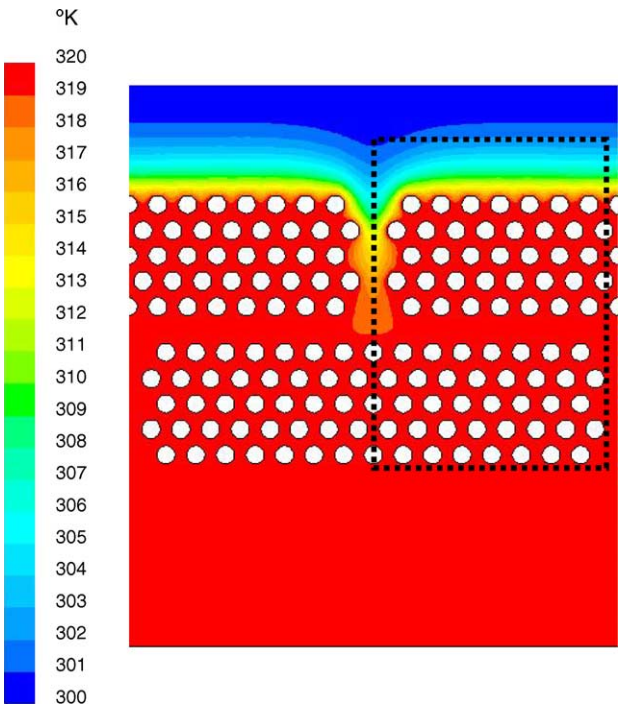

Fig. 8. The temperature distribution on the model of the glass fabric. The dotted line rectangle is a histogram area (see Fig. 9).

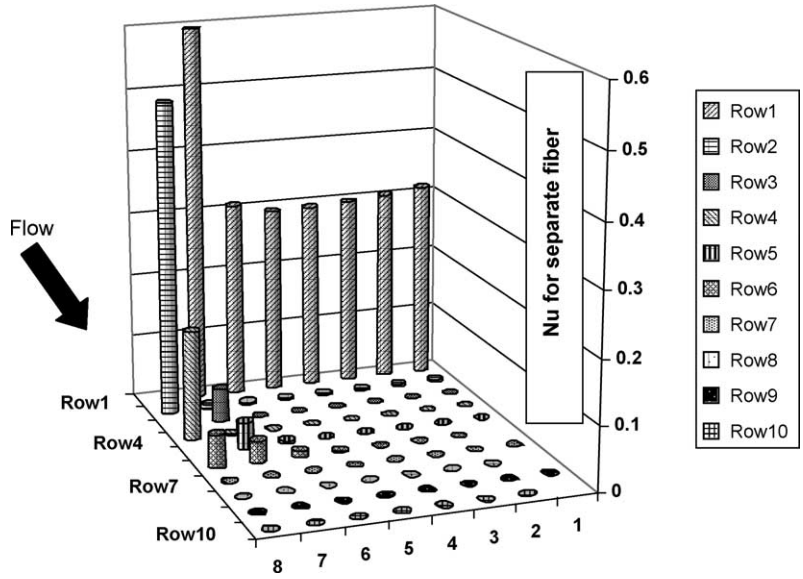

Fig. 9. Distribution of Nu criterion for separate fibers in the marked area of yarn cross-section (see Fig. 8).

The chosen comparatively simple geometric model of the woven fabric based on two geometrical parameters, i.e., diameter of a fiber in the yarn and characteristic size of the transport channel, is satisfactory to obtain data on the heat transfer between the woven fabric and the filtered flow.

Criterial dependencies for heat and mass transfer parameters usually are interpolated in terms of the following expressions: $\mathrm{Nu} = A \times Re^n \times \mathrm{Pr}^{1/3}$; $\mathrm{Sh} = A \times Re^n \times \mathrm{Sc}^{1/3}$. The log plots in Fig. 10 demonstrate that the criterial dependencies for the woven fabric in the range of filtration rates under study are impossible to interpolate if identical constants A and n are used. For more precise data interpreting, the Nu(Re) dependence should be divided into three regions with related A and n constants (see Fig. 11). The values for pre-exponential factor A and exponent n are given in Table 2.

The fact that the criterial dependence Nu(Re) (or Sh(Re)) cannot be formulated in terms of a single interpolation expression 15 (Appendix A) results in inevitable discrepancy between the experimental and literature data (see Fig. 5). The results discussed in the present work are obtained for the case of comparatively low rates and small Reynolds numbers $Re < 5$, Re being determined from the diameter of fibers in the yarn. The literature data on Nu(Re) [5,6] relate to the rate ranges and, correspondingly, to the Reynolds numbers $Re \gg 50$ that are most characteristic of heat engineering and hydrodynamics. When these dependencies are extrapolated to the region of small Reynolds numbers, the experimental data differ from the data reported in Refs. [5,6].

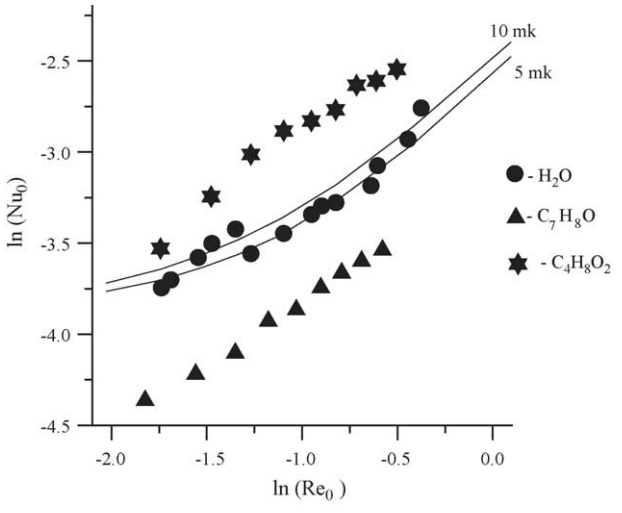

Fig. 10. Comparison of heat exchange characteristics $\mathrm{Nu}_0(Re_0)$. The data are obtained with the CFD Fluent software (solid lines) and calculated from experimental data for water, dioxane and benzyl alcohol (symbols).

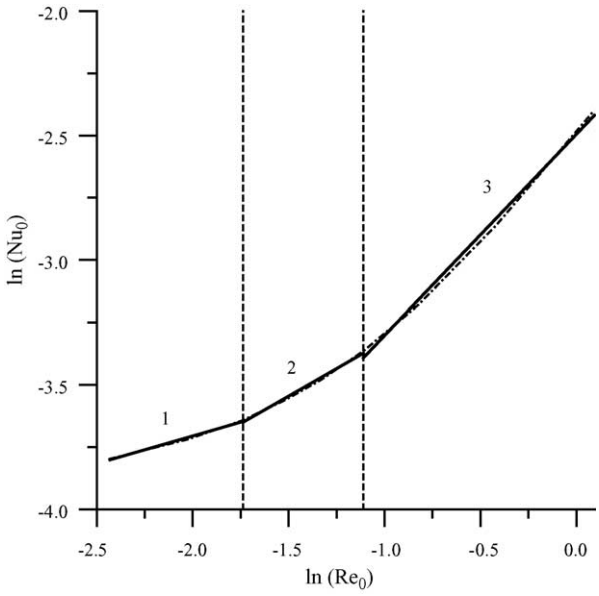

Fig. 11. Log plots of interpolated dependencies Nu(Re).

Table 2
Constants in criterial function Nu(*Re*)

	Rate range (m/s)	*A*	*n*
1	0.2–0.4	0.038	0.22
2	0.4–0.75	0.056	0.45
3	0.75–2.5	0.083	0.81

5. Conclusions

1. Mass transfer processes in a glass fabric sample are studied using NMR tomography. The uniqueness of the method is that the surface processes can be in situ studied at a sufficient experimental accuracy. As a result, the rates R_0 of fluid evaporation from the woven support surface are experimentally determined.
2. A one-dimensional mathematical model is proposed for processing of the experimental data which allows mass transfer criteria Sh = Sh(*Re*) to be calculated at the stationary evaporation conditions. The results obtained are compared to the dependencies known from literature on parallel cylinder rows and woven metal gauzes at $Re > 1$.
3. The CFD FLUENT software package is used to create a numerical model in order to take into account the local hydrodynamics of the flow passing around the fibers in the yarns of the woven fabric. The hydrodynamics of the filtered flow is studied at small *Re* numbers and parameters are determined for heat transfer between the yarns and the flow. The inner fibers in the yarn are shown practically not to participate in the heat and mass transfer processes. The calculated and experimental results are compared. A good agreement is shown between the results obtained by both calculation procedures.
4. Inspection of the results allows at least three regions to be identified in the curve, where the criterial dependence Nu(*Re*) may involve different coefficients.

Appendix A. Mathematical model formulation

The stationary process of a fluid evaporation from a sample surface is described by an equation set:

$$\alpha \times S_{ud} \times (\theta - T) = -\Delta H \times R(z); \tag{A.1}$$

$$u\rho \times C_\mathrm{p} \times \frac{\mathrm{d}T}{\mathrm{d}z} = \lambda \frac{\mathrm{d}^2T}{\mathrm{d}z^2} - S_{ud}\alpha \times (T - \theta); \tag{A.2}$$

$$\beta \times S_{ud} \times (C - C_\mathrm{S}) = -R(z); \tag{A.3}$$

$$u\frac{\mathrm{d}C}{\mathrm{d}z} = D\frac{\mathrm{d}^2C}{\mathrm{d}z^2} - \beta \times S_{ud} \times (C - C_\mathrm{S}) \tag{A.4}$$

$$\frac{\alpha}{\beta} = \left(\frac{\mathrm{Sc}}{Pr}\right)^{2/3} \times \frac{C_\mathrm{p}(\hat{T})}{8.21 \times 10^{-5} \times \hat{T}} \tag{A.5}$$

$$C_\mathrm{S} = C_\mathrm{S}(\theta) \tag{A.6}$$

The boundary conditions are:

$$C|_{z=0} = 0; \quad T|_{z=0} = T_0; \quad \left.\frac{\mathrm{d}C}{\mathrm{d}z}\right|_{z=L} = 0; \quad \left.\frac{\mathrm{d}T}{\mathrm{d}z}\right|_{z=L} = 0. \tag{A.7}$$

The model is based on the following assumptions:

(1) Axis z coincides with the vector of initial gas flow rate and is perpendicular to the sample surface;
(2) Heat conductivity of the solid phase (glass fabric) equals zero;
(3) When mass transfer processes between gas and the fibrous support are described, the longitudinal heat conductivity and gas phase diffusion are taken into account. The characteristic size of the woven fabric layer being small enough (of the order of several millimeters), these processes may contribute considerably. The heat conductivity of the gas mixture (this is the case of air) is determined by formula:

$$\lambda(\hat{T}) = \frac{\nu(\hat{T})}{0.7} \times C_\mathrm{p}(\hat{T}) \times \frac{1}{8.21 \times 10^{-5} \times \hat{T}} (\mathrm{J/ms\,deg}) \tag{A.8}$$

where

$$\nu(\hat{T}) = \nu_0 \times \left(\frac{\hat{T}}{273^\circ}\right)^{1.75},$$
$$(\nu_0 = 1.33 \times 10^{-5} (\mathrm{m^2/s}) \text{ for air}) \tag{A.9}$$

The coefficient of fluid air diffusion in air is calculated by formula:

$$D(\hat{T}) = D_0 \times \left(\frac{\hat{T}}{273^\circ}\right)^{1.75}, \tag{A.10}$$

(4) Concentration of the fluid vapor on the glass fabric surface equals the saturated concentration at the temperature identical to the fabric surface temperature. The concentration as a function of temperature (Eq. (A.6)) is determined with the Antoine equation for partial pressures of saturated fluid vapors [6]. While the concentration of fluid vapor in the gas is low, the following formula can be used to calculate the temperature dependence of specific heat capacity of air:

$$C_\mathrm{p}(\bar{T}) = 28.3 + 0.00254 \times \bar{T} + 0.574 \times 10^{-6} \times \bar{T}^2 (\mathrm{J/(mol \times deg)}) \tag{A.11}$$

(5) Specific surface area of the woven fabric is determined from the external surface of all fibers per 1 $\mathrm{m^3}$ of the fabric:

$$S_{ud} = \frac{S_\Sigma}{V} \tag{A.12}$$

(6) Coefficients of heat and mass transfer are constant through the layer thickness. They are calculated

by formulae:

$$\alpha = \mathrm{Nu} \times \frac{\lambda(\hat{T})}{d}\,(J/\mathrm{m}^2\,\mathrm{s\,deg}) \tag{A.13}$$

$$\beta = \mathrm{Sh} \times \frac{D(\hat{T})}{d}\,(\mathrm{m/s}) \tag{A.14}$$

The coefficients are determined at the mean temperature, $\hat{T} = (\bar{T} + \bar{\theta})/2$.

Criterial laws of convective heat and mass transfer are approximated by similar formulae:

$$\mathrm{Nu} = A \times Re^n \times \mathrm{Pr}^{1/3}; \quad \mathrm{Sh} = A \times Re^n \times \mathrm{Sc}^{1/3} \tag{A.15}$$

This implies a relationship between coefficients α and β:

$$\frac{\alpha}{\beta} = \left(\frac{\mathrm{Sc}}{\mathrm{Pr}}\right)^{2/3} \times \frac{C_\mathrm{p}(\hat{T})}{8.21 \times 10^{-5} \times \hat{T}} \tag{A.16}$$

Note that the Prandtl number for air can be Pr = 0.7, while the Schmidt number is determined by relationship:

$$\mathrm{Sc} = \frac{\nu(\hat{T})}{D(\hat{T})} \tag{A.17}$$

The Reynolds number is calculated by formula:

$$Re = \frac{u \times d}{\nu(\hat{T}) \times \varepsilon} \tag{A.18}$$

where a yarn diameter (d = 0.75 mm) or the diameter of an individual fiber (d_0 = 6.5 μm) can be used as the characteristic size.

(7) The fabric layer thickness is $L = 2d$.

(8) The local evaporation rate $R(z)$ as a term in Eqs. (A.2) and (A.4) is unknown but its thickness averaged magnitude (L) is assumed to correspond to the experimental value:

$$\bar{R} = \frac{1}{L}\int_0^L R(z)\,\mathrm{d}z = R_0 \tag{A.19}$$

The numerical solution of the non-linear set of differential Eqs. (A.1)–(A.6) is found based on some simplifications. The solid phase temperature $\theta(z)$ and surface concentration $C_\mathrm{S}(z)$, which are in relationship through Eq. (A.6), can be expressed as functions of gas phase temperature and concentrations (Eqs. (A.1) and (A.3) are used). Mass transfer coefficient β also can be expressed using these values (from Eq. (A.3) when layer length integrated).

Based on the simplified data, solution of the original problem is reduced to the numerical solution of the boundary problem formulated for the system of two second-order nonlinear ordinary differential equations with respect to unknown functions $T(z)$ and $C(z)$ (Eqs. (A.2) and (A.4)). While the equation set is resolved for given gas flow rates u, the related mass transfer coefficients $\beta(u)$, and consequently $\mathrm{Sh}(u)$, can be determined.

References

[1] Yu. Matatov-Meytal, M. Sheintuch, Appl. Catalysis A: General 231 (2002) 1–16.
[2] L. Apelbaum, M. Temkin, Phys. Chem. J. 22 (2) (1948) 195–207.
[3] B.S. Bal'zhinimaev, L.G. Simonova, V.V. Barelko, A.V. Toktarev, V.I. Zaikovskii, V.A. Chumachenko, Chem. Eng. J. 91 (2003) 175–179.
[4] B.S. Petukhov, Heat-exchanger hand-book, vol. 1, M: Energoatomizdat, 1987. pp. 247–251.
[5] V.V. Barelko, Eng. Phys. J. 21 (1) (1971) 78.
[6] R.C. Reid, T.K. Sherwood, The Properties of Gases and Liquids, in: V.B. Kogan (Ed.), Chemistry, Leningrad, 1971, p. 704.